Characterization of a New Composite Material: Fe_2O_3-Impregnated Poly(tetrafluoroethylene). Particle Size Determination and Photoacoustic Spectroscopy

F. GALEMBECK, *Instituto de Quimica da Universidade de São Paulo, São Paulo, Brasil,* C. C. GHIZONI, *CNPq-INPE, São José dos Campos, SP, Brasil,* and C. A. RIBEIRO, H. VARGAS, and L. C. M. MIRANDA, *Instituto de Física da Universidade Estadual de Campinas, Campinas, SP, Brasil*

Synopsis

Iron carbonyl sorption in PTFE, followed by *in situ* oxidation, gives the composite material, iron oxide–PTFE. Oxide particle size determination was performed by electron microscopy. The particles were found to be nearly spherical and very small, having diameters in the 30–40 Å range on average. Optical absorption spectra were obtained by photoacoustic spectroscopy, and their intensities show a complex dependence on iron oxide concentration in the samples.

INTRODUCTION

Poly(tetrafluoroethylene) (PTFE) is a highly inert and practically insoluble polymer of chemical formula $(-CF_2-)_n$ which has considerable technological importance.[1] PTFE resists attack by the most aggressive chemical agents, with the exception of metallic sodium[2] and alkalies[3,4] under extreme conditions. In addition, it is highly immiscible with most solids and liquids. This combination of properties is a serious obstacle to the development of useful composite materials in which PTFE is a component. We have found that a new approach can be successfully applied to this problem, leading to new materials such as iron(III) oxide-impregnated PTFE discussed in this article.

Our approach is based on the fact that metalorganic substances with sufficiently low solubility parameters are predicted by Hildebrand's theory of regular solutions[5] to be miscible with PTFE. Once the metal-organic compound is absorbed by the polymer, it can be made to react to yield other substances. In the present case, iron pentacarbonyl, $Fe(CO)_5$, was absorbed in PTFE and subsequently transformed in iron oxide, thus generating the new material, composite PTFE–iron oxide. Since the individual components of this composite exhibit highly contrasting properties, one would expect that such features would be reflected in the properties of the composite. For instance, we have found previously that a dramatic change in the adsorbent properties of PTFE occurs upon its surface modification by incorporation of the iron oxide.[6]

In this article, we describe the preparation of the composite PTFE–iron oxide; oxide particle size determination was performed by electron microscopy on composite samples. Absorption spectra were obtained using the technique of photoacoustic spectroscopy.

Journal of Applied Polymer Science, Vol. 25, 1427–1433 (1980)

0021-8995/80/0025-1427$01.00

EXPERIMENTAL

Sample Preparation

PTFE samples were 0.2-mm-thick sheets, fabricated from du Pont Teflon by Incoflon (São Paulo). The identity and purity of the material was checked by melting point measurement, infrared spectrophotometry, and electron spectroscopy (ESCA). The degree of crystallinity of the original material, determined by x-ray diffraction, was 65%. After thermal annealing (2 hr at 206°C), the degree of crystallinity was found to be 70%. Iron pentacarbonyl was obtained from Alpha Inorganics and distilled prior to use.

The PTFE samples were thoroughly washed with ethanol and dried under vacuum. After weighing, the samples were immersed in a 10% solution of $Fe(CO)_5$ in ethanol at room temperature. Under these conditions, the carbonyl is absorbed by the polymer but ethanol is not.[7] PTFE samples were left soaking for varying periods of time; after removal from the liquid, they were irradiated in the beam of a slide projector, under which conditions the nonvolatile diiron eneacarbonyl is formed.[8] The samples were then allowed to undergo complete oxidation under air. After three days, each sample was heated to 105°C to eliminate remaining traces of unreacted iron carbonyl. This elimination was monitored by IR spectrophotometry. The samples were then washed with 1*N* sulfuric acid and ethanol and air dried to constant weight. The iron oxide content was determined by weighing the samples after completing the incorporation procedure and was also gravimetrically checked following thermal decomposition of the PTFE. The iron oxide contents in the samples ranged from 0.34 to 1.50% (w/w).

Oxide Particle Size Determination

Iron oxide particle size determination was performed in a Hitachi HU12 transmission electron microscope. The samples were subjected to mechanical slicing, followed by electron bombardment under vacuum in the microscope to make them sufficiently thin for adequate transmission imaging. Pictures of the thinner regions were analyzed assuming that the oxide particle sizes did not change during this treatment (i.e., that the only change caused by this treatment was the depolymerization of PTFE and evaporation of monomeric C_2F_4).

The particles appeared very close to spherical in the microphotographs; some particle-size histograms are presented in Figures 1 and 2.

Optical Absorption

In this section, we present the results of optical absorption measurements performed on the PTFE–iron oxide samples. Conventional UV-visible spectrophotometry failed to give reliable data because of the opacity of the samples. We have thus resorted to the photoacoustic technique which is well suited to the study of crystalline, powdered, and amorphous solids.

The experimental setup used consists of a 200-W tungsten filament lamp, a variable-speed light chopper, a monochromator, an air-filled aluminum cell with a condenser microphone, a low-noise preamplifier, and a lock-in amplifier. The sample compartment is a cylindrical chamber with a diameter of 1 cm; 1-cm discs

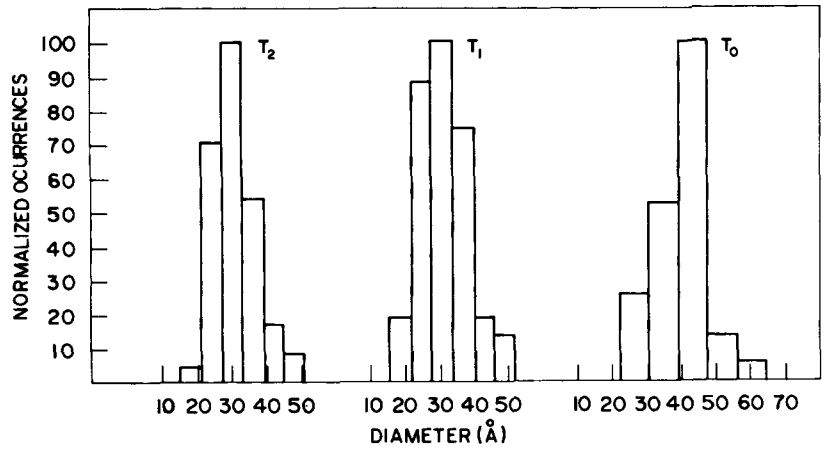

Fig. 1. Fe_2O_3 particle size histogram for the lower concentration samples.

of iron oxide–PTFE were weighed to correct for differences in masses between the samples.[9]

Using powdered charcoal as a nearly perfect absorber, the fraction of the incident signal absorbed by the samples was calculated as

$$\text{normalized absorption} = \frac{\text{sample signal} - \text{undoped matrix signal}}{\text{charcoal signal}}$$

Optical absorption spectra of typical samples are illustrated in Figure 3. In Figure 4, we give the dependence of the relative peak absorption signal (in the 3500–4000 Å region) on the oxide concentration of the samples.

The spectra given in Figure 3 exhibit strong absorption bands which are most readily attributable to charge transfer from oxygen to a central iron(III) ion in an octahedral configuration.[10]

The dependence of the photoacoustic signal, taken at the maximum peak absorption (in the 3500–4000 Å region) on the concentration of Fe_2O_3 particles (Fig. 4), suggests the existence of two different volume distributions for the samples examined. This conclusion is arrived at by taking into account the

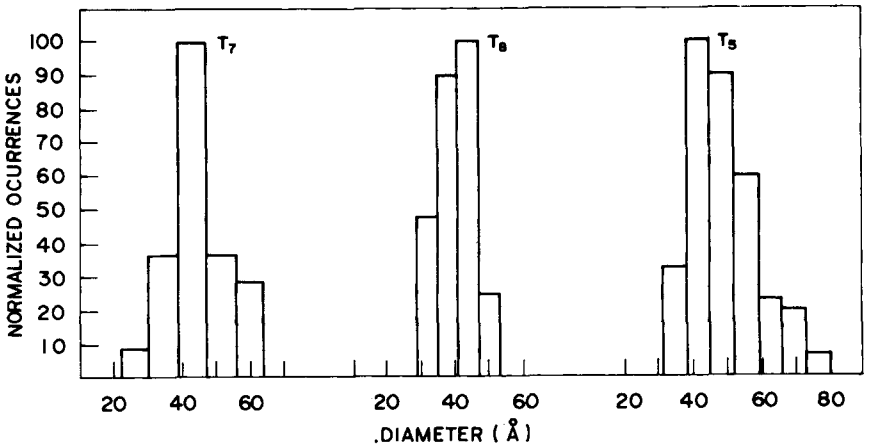

Fig. 2. Fe_2O_3 particle size histogram for the higher concentration samples.

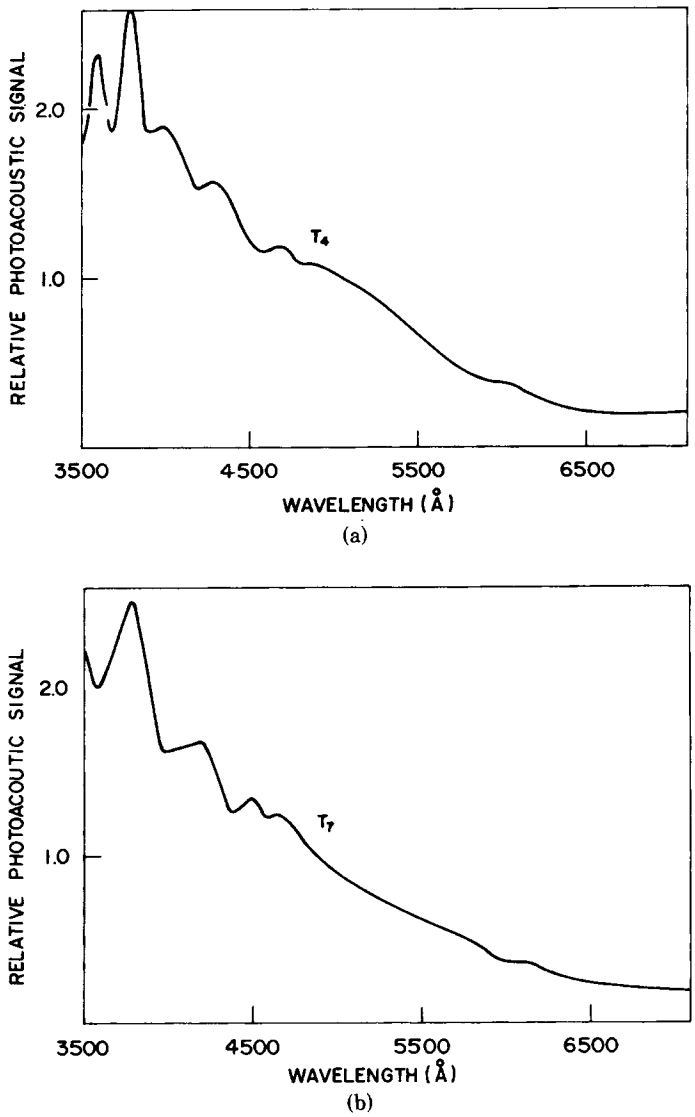

Fig. 3. (a) Relative absorption spectrum for sample T_4 (c = 0.94%). (b) Relative absorption spectrum for sample T_7 (c = 1.39%).

physical processes involved in the photoacoustic effect. The acoustic signal is, in general, produced by the sum of contributions of both bulk and surface radiation absorption to heat generation.[11–14] In the case of optically opaque samples,[12–14] the signal does not depend explicitly on the bulk optical absorption coefficient but still remains explicitly dependent upon the surface absorption coefficient. Since any absorption coefficient should be proportional to the concentration of absorbers, one should then expect that for an optically opaque sample with a nonvanishing absorption at the surface the photoacoustic signal is a linear function of concentration c with a finite value extrapolated to the origin (c = 0). This extrapolated value is due to the absorption at the solid bulk. Furthermore, if the sample is thermally thick, as in the present case, it can be

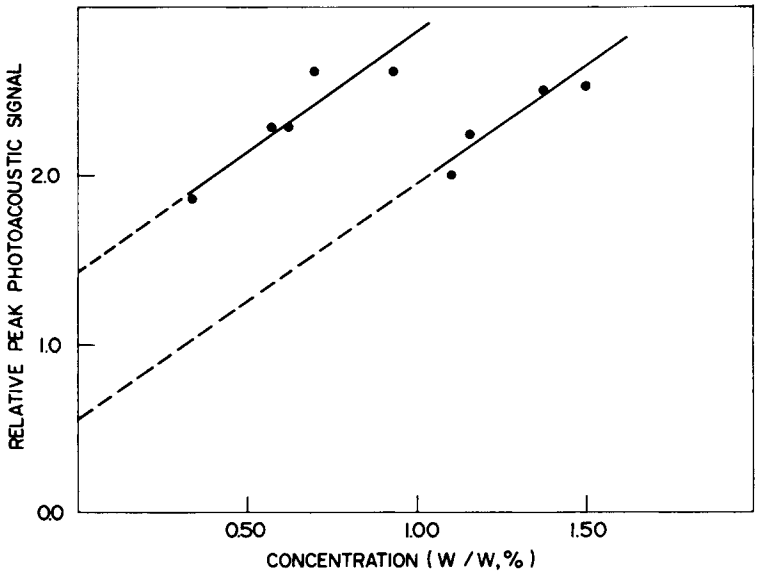

Fig. 4. Relative photoacoustic signal at the maximum absorption peak vs. concentration of the samples.

shown that the bulk contribution should be proportional to the surface thermal conductance.[11,12] Hence, the expression for the complex pressure fluctuations δP in the gas owing to absorption by an optically opaque and thermally thick sample can be written as,[12,13]

$$\delta P = \frac{A_g}{f}\left(\frac{He^{-j\pi/4}}{(2\pi f\rho_s c_s k_s)^{1/2}} + \beta'\right)\exp\left[j\left(\omega t - \frac{\pi}{4}\right)\right] \tag{1}$$

where A_g is a constant which depends only on the gas (air) thermal properties; f is the chopping frequency; k_s, ρ_s, and c_s are, respectively, the thermal conductivity, the density, and the specific heat of the sample; and β' and H are the surface optical absorption coefficient and the surface thermal conductance, respectively.

The above expression can be used to interpret our data, assuming that β' is proportional to c and that the surface thermal conductance is inversely proportional to the area of the oxide particles, multiplied by N, the number of oxide particles at the surface. Thus, we take $H \sim 4N/\pi d^2$. Here we note that even in the case of an homogeneous solid there is no simple analytical expression for the surface thermal conductance,[15,16] and for most purposes one usually depends on empirical determinations of H. Hence, assuming the validity of the previously discussed model and considering that $N = 4 \times$ (PTFE cross section)$/\pi d^2$, where d is the average oxide particle diameter, we have

$$H = h/d^4 \tag{2}$$

where h is a proportionality constant. Combining eqs. (1) and (2), we have

$$\delta P = A/d^4 + cB \tag{3}$$

In eq. (3), the first term on the right-hand side represents the volume contribution to the photoacoustic signal, whereas the second term gives the surface

contribution, which is shown to have a linear dependence on the concentration.

The existence of the two straight lines in Figure 4 may therefore be associated with the formation of two characteristic volume distributions of iron oxide particles, each prevailing in a given concentration range. This can be seen by comparing the ratio of the two intercepts in Figure 4 to the ratio of the inverse mean diameters to the fourth power. From the electron microscopy data given in Table I, we have $\bar{d}_1 = 36$ Å and $\bar{d}_2 = 44$ Å, where subscripts 1 and 2 refer to points in the upper (lower) straight line in Figure 4. Thus, $(\bar{d}_2/\bar{d}_1)^4 = 2.2$, in good agreement with the ratio of the intercepts, equal to 2.6.

It should be mentioned that the above discussion was based upon the hypothesis of the bulk thermal properties of the composite showing little dependence on iron oxide particle concentration in the range studied. The parameter A in eq. (3) varies with $(k_s c_s)^{-1/2}$, and we have assumed that it is independent of the concentration. This is verified by the results in Figure 4: a straight-line dependence is observed for each particle population, and the slopes of both straight lines are identical, within experimental error.

CONCLUSIONS

Sorption and *in-situ* reaction can be used to obtain a PTFE–iron oxide composite. Although the components of this system are usually considered incompatible, the composite material is obtained using mild, reproducible, and standard chemical methods. The material obtained is stable under room conditions, showing no tendency to phase separation, embrittlement, etc. Indeed, we have found that the oxide may be used to anchor other chemicals and incorporate them in the PTFE, leading to other derivatives (Galembeck et al., to be published).

Iron oxide particles, obtained as nearly spherical, ultrafine particles, are rather uniform in size. Particles are larger in the more concentrated samples.

Photoacoustic spectroscopy yielded optical absorption spectra of the samples. The signal intensity has a complex dependence on sample oxide concentration, which can be understood assuming that the acoustic signal has two components, one arising from absorption at the bulk, the other from absorption at the surface.

TABLE I
Summary of Electron Microscopy Data for Samples Examined

Sample	Concentration, %	Average diameter, Å	Peak diameter, Å	Spread FWHM (full width half maximum of distribution), Å
T_0	0.34	44.2	44	12
T_1	0.58	30.4	30	16
T_2	0.62	30.8	29	13
T_3	0.70	39.9	—	—
T_4	0.94	—	—	—
T_5	1.10	49.6	44	20
T_6	1.16	—	—	—
T_7	1.39	44.2	43	13
T_8	1.50	40.2	42	16

Furthermore, the surface thermal conductance is assumed to be proportional to the square of the area of the oxide particles. The results given show the potential usefulness of photoacoustic spectroscopy in the study of polymers.

One of the authors (F. G.) acknowledges the support of FAPESP (Grant No. 77/355), and all the authors want to thank Professor S. Caticha Ellis who made available the facilities of his electron microscopy laboratory.

References

1. C. A. Sperati and H. W. Starkweather, Jr., *Fortschr. Hochpolym.-Forsch.*, **2,** 465 (1962).
2. D. W. Dwight and W. M. Riggs, *J. Colloid Interface Sci.*, **47,** 650 (1974).
3. H. Fitz and F. Mayer, Germ. Pat. 2,354,210 (1975); *Chem. Abstr.*, **83,** 148344 (1975).
4. N. I. Egorenkov, D. A. Rodchenko, A. I. Barki, and V. V. Kumareva, USSR Pat. 458,567 (1975); *Chem. Abstr.*, **83,** 60935g (1975).
5. J. H. Hildebrand and R. L. Scott, *The Solubility of Non-Electrolytes,* 3rd ed., Reinhold, New York, 1950, p. 40.
6. F. Galembeck, *J. Polym. Sci. Polym. Lett. Ed.*, **15,** 107 (1977).
7. F. Galembeck, S. E. Galembeck, H. Vargas, C. A. Ribeiro, L. C. Miranda, and C. Ghizzoni, in *Surface Contamination,* K. L. Mittal, Ed., Plenum, New York, 1979.
8. F. Galembeck, *J. Polym. Sci. Polym. Chem. Ed.*, **16,** 3015 (1978).
9. M. J. Adams, A. A. King, and G. F. Kukbright, *Analyst,* **101,** 73 (1976).
10. P. Day and C. K. Jorgensen, *J. Chem. Soc.*, 6226 (1964).
11. H. S. Bennett and R. A. Forman, *Appl. Opt.*, **15,** 2415 (1976); **16,** 2834 (1977); *J. Appl. Phys.*, **48,** 1432 (1977).
12. C. L. Cesar, H. Vargas, J. A. Meyer, and L. C. M. Miranda, *Phys. Rev. Lett.*, **42,** 1560 (1979).
13. C. A. S. Lima and L. C. M. Miranda, paper presented at the Photoacoustic Conference, Ames, IA, August 1–3, 1979.
14. A. Rosencwaig and A. Gersho, *J. Appl. Phys.*, **47,** 64 (1976).
15. V. S. Arpaci, *Conduction Heat Transfer,* Addison-Wesley, Reading, MA, 1966.
16. H. S. Carslaw and J. C. Jaeger, *Conduction of Heat in Solids,* Clarendon, Oxford, 1959.

Received February 22, 1979
Revised January 4, 1980